International Journal of Concrete Structures and Materials
Vol.18, No.1E, pp.17~22, June 2006

Corrosion Resistance of Cr-Bearing Rebar to Macrocell Corrosion Environment Induced by Localized Carbonation

Sung-Ho Tae[1)]

(Received December 31, 2005, and accepted May 26, 2006)

Abstract: Artificial cracks were made in the cover concrete of specimens embedding ten types of steel rebars of different Cr contents. The research aims for developing Cr-bearing steel rebars resistant to macrocell corrosion environments induced by cracking in cover concrete. The cracks were subjected to intensive penetration of carbon dioxide (carbonation specimens) to form macrocells. The carbonation specimens were then treated with accelerated corrosion curing, during which current macrocell corrosion density was measured. The corrosion area and loss from corrosion were also measured at the end of 105 cycles of this accelerated curing. The results of the study showed that Cr-bearing steel with Cr content of 5% or more suppressed corrosion in a macrocell corrosion environment induced by the differences in the pH values due to carbonation of cracked parts. Cr-bearing steels with Cr content of 7% or more are proven to possess excellent corrosion resistance.

Keywords: Cr-bearing rebar, corrosion resistance, macrocell corrosion, carbonation, crack.

1. Introduction

When cracked for any reason, concrete surfaces become vulnerable to penetration by corrosion factors, such as carbon dioxide, chloride ions, oxygen, and moisture. When these factors exceed the corrosion threshold of a pH value of 12.5, reinforcement corrosion begins to develop. Generally, the seepage of corrosion factors through the passage of cracking in concrete surfaces is significantly faster than that through sound surfaces,[1,2] causing macroscopic heterogeneity of the reinforced concrete cover, thereby inducing macrocell corrosion of the reinforcement. Macrocell corrosion refers to concentrated corrosion that occurs when concrete or reinforcement surfaces become heterogeneous, forming anodic and cathodic areas. Investigation against macrocell corrosion is crucial for the evaluation of the durability of reinforced concrete, as macrocell corrosion proceeds more rapidly than microcell corrosion and tends to go deeper into a small area. For this reason, a large number of studies have conventionally been conducted regarding the reinforcement corrosion induced by cracking of the cover concrete.[3-6] For this reason, many studies have been carried out to find out the best method for preventing corrosion in reinforcing bars. However, most of these researches have been disproportionately concentrated on the improvement of concrete quality, eg. increase in concrete cover thickness, optimization of water-to-cement ratio or the addition of corrosion resistant materials. In America and Europe, epoxy-coated rebars[7,8] and stainless steel rebars[9-11] with high corrosion resistance have already been applied to many concrete structures. Nevertheless, epoxy-coated rebars have certain drawbacks. They cause losses in the bond strength with concrete and are prone to bending, damage during transportation and fabrication, thereby being rendered vulnerable to macrocell corrosion. On the other hand, stainless steel rebars have excellent properties as corrosion resistant rebars, but their higher cost prevents from being used widely. With this as a background, the author has reported the corrosion-inhibiting properties of Cr-bearing reinforcing bars in concrete under a microcell corrosion environment in a previous paper[12] with the aim for developing Cr-bearing rebars that have lower alloy element content (chromium, nickel, molybdenum, etc.) than general stainless steel. The proposed Cr-bearing rebars would be corrosion-resistant while being producible with the same process flow as normal steel.

This paper reports on a study on the corrosion-inhibiting properties of Cr-bearing rebars under a macrocell corrosion environment induced by cracking in cover concrete. It is a part of the research and development effort for Cr-bearing rebars, which have the corrosion-inhibiting properties. This property is required in specific corrosion enviroments, to which reinforced concrete structures are often exposed. Accordingly, reinforced concrete specimens were fabricated with artificial cracks in the cover concrete. These specimens were then subjected to intensive penetration of carbon dioxide through such cracks to induce macrocell corrosion (hereafter referred to as carbonation specimens). Accelerated corrosion testing was then conducted on these specimens to measure their half-cell potential, macrocell corrosion current, corrosion area, and corrosion loss.

2. Outline of experiment

Ten types of rebars having different Cr contents were embedded

[1)] KCI member, Dept. of Architectural Engineering, Sustainable Building Research Center, Hanyang University, Ansan 426-791, Korea.
E-mail: jnb55@hanyang.ac.kr,

in concrete with a cover depth of 20 mm. Each specimen had two types of rebars with the upper and lower bars on the same side being of the same type for a total of four rebars per specimen. Stainless steel plates of 0.5 mm in thickness were transversely inserted from the top and bottom of each specimen to the depth of the bars as shown in Fig. 1. After sealed curing for 24 hours, the specimens were demolded, and the stainless steel plates were removed to leave gaps imitating simulating cracks. The specimens were then placed in plastic bags for further sealed curing for seven days. Carbonation specimens were then air-cured for one month in a thermo-hydrostatic room ($20 \pm 3^{\circ}C$ and $50 \pm 5\%$ R.H.), and they were subjected to accelerated carbonation so that carbonation would occur only in concrete near the cracks. This was followed by accelerated corrosion curing, in which each two-day cycle consisted of one day at high temperature and high humidity ($60^{\circ}C$ and 95% R.H.) and the other day at low temperature and low humidity ($30^{\circ}C$ and 50% R.H.). The changes in the macrocell corrosion current were measured up to 105 cycles, at the end of which the half-cell potential, corrosion area, and corrosion loss of the anodic and cathodic rebars were measured. Fig. 2 shows the test setup. Tables 1 and 2 show the material properties and mixture proportions of concrete, respectively. The reinforcing bars were round-shaped with a diameter of 13 mm, from which the mill scale was removed before use. The basic compositions of reinforcing bars are similar to Table 3.

3. Experiment procedure

3.1 Accelerated carbonation testing

Accelerated carbonation tests were conducted on carbonation specimens. Except for the area (width = 10 mm) on each side of the artificial crack, the concrete surfaces were covered with a packing tape and then coated with epoxy as shown in Fig. 3. This taping and coating were necessary to carbonate only the area near the crack and to prevent CO_2 penetration through other surfaces.The conditions for accelerated carbonation were temperature of $40^{\circ}C$, relative humidity of 60%, and CO_2 concentration of 5%. The degree of carbonation was judged by cutting through the cracks of the specimens to measure the carbonation depth every month by spraying a 1% alcoholic solution of phenolphthalein onto the cut surface. The uncolored part of concrete was the carbonated part, and its depth was measured. Accelerated carbonation testing was

Table 1 Material properties.

Materials	NaCl
Cement	Ordinary Portland Cement
Water	Potable
Fine aggregate	Crushed Sand and Land Sand/Density = 2.52 ton/m^3, Absorption = 1.42 %, Fineness Modulus = 2.73 %
Coarse aggregate	Crushed Stone (Sand Stone)/Density = 2.64 ton/m^3, Absorption = 0.59 %, Fineness Modulus = 6.75 %
Chemical admixture	Air entraining and high-range water reducing agents
NaCl	First class reagent

Table 2 Mixture proportions of concrete.

W/C	S/A	Slump	Unit weight (kg/m^3)			
(%)	(%)	(cm)	W	C	S	G
65	46	18	185	285	798	954

Table 3 Chemical compositions of steels, mass%.

Steel	C	Si	Mn	P	S	Cr	Ni	Mo
SD345	0.2190	0.300	1.34	0.035	0.019	0.081	0.04	0.01
0Cr	0.0117	0.300	0.50	0.031	0.005	0.011	0	0
3Cr	0.0106	0.305	0.52	0.033	0.006	3.070	0	0
5Cr	0.0112	0.266	0.52	0.030	0.005	4.880	0	0
7Cr	0.0105	0.270	0.53	0.031	0.005	7.150	0	0
9Cr	0.0114	0.270	0.52	0.029	0.005	9.070	0	0
11Cr	0.0098	0.276	0.52	0.030	0.005	11.110	0	0
13Cr	0.0108	0.270	0.51	0.029	0.006	12.900	0	0
16Cr	0.0094	0.270	0.53	0.030	0.005	16.090	0	0
SUS304	0.0620	0.297	1.02	0.030	0.006	18.280	8.15	0.051

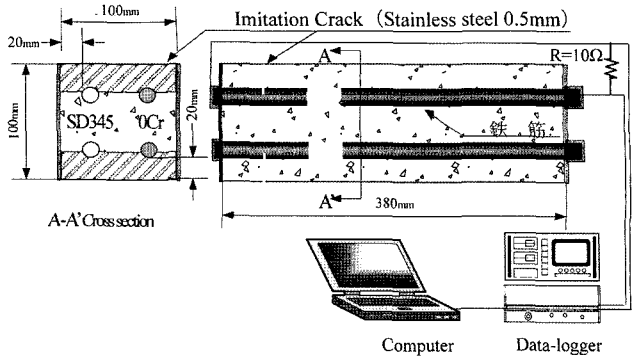

Fig. 1 Details of test specimen.

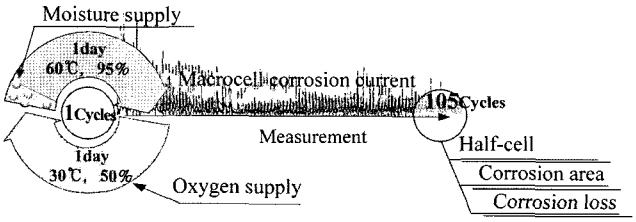

Fig. 2 Test setup.

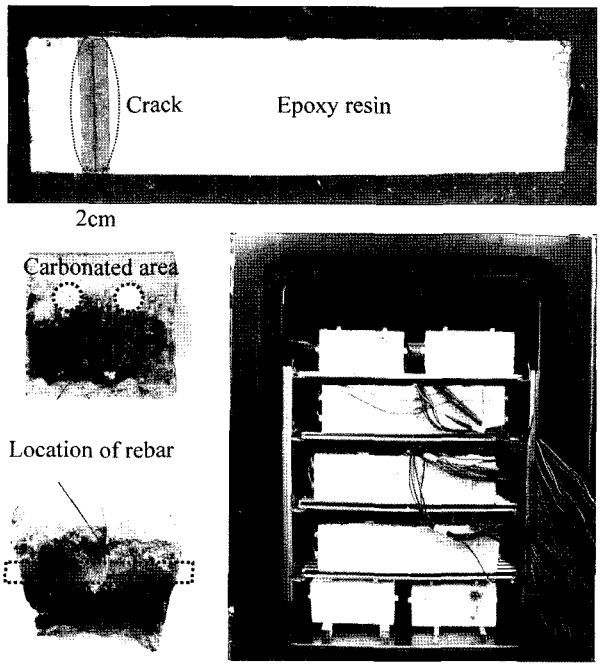

Fig. 3 Accelerated carbonation.

terminated three months after carbonation had developed through the 20 mm cover and reached well behind the bars. The specimens were then stripped of the packing tape and subjected to accelerated corrosion curing with high temperature/high humidity and low temperature/low humidity cycles.

3.2 Accelerated corrosion curing

Carbonation specimens were subjected to accelerated corrosion curing by temperature and humidity cycles consisting of high temperature and high humidity conditions (60°C and 95% R.H.) for one day and low temperature and low humidity conditions (30°C and 50% R.H.) for one day.

3.3 Macrocell corrosion current

The macrocell corrosion current was measured once every one hour by measuring the voltage between the anodic bars and cathodic bars via a known resistance of 10 Ω. An automatic measurement system consisting of a switch box, a data logger, and personal computer was used as shown in Fig. 1. The value was then converted to the macrocell corrosion current based on Ohm's law.

3.4 Half-cell potential

The half-cell potentials of chloride attack specimens and carbonation specimens were measured on the surfaces of cover concrete for anodic and cathodic rebars at the end of 105 cycles of accelerated corrosion curing. Saturated copper-copper sulfate electrodes (CSE) were used as the counter electrodes. The specimens were sprayed with water immediately before measurement to adjust their moisture content.

3.5 Corrosion area and corrosion loss

At the end of 105 cycles of accelerated corrosion curing, anodic and cathodic rebars were chipped out of the carbonation specimens, and their corrosion areas, and then calculating the corrosion area with a software for automatic area measurement. The weight loss was measured in accordance with Japan Concrete Institute Standard.[13] Rust was removed from the bars by immersing the SD345, 0Cr, and 5Cr bars in a 10% diammonium citrate solution, whereas a 15% nitric acid solution was used for bars with a Cr content exceeding 5%. The masses of the bars were measured to the accuracy of 0.01 g with an electronic balance, and the weight loss was determined by Eq. (1) below.

$$\Delta W = \frac{(Wo - W) - Ws}{Wo} \times 100 \quad (1)$$

Where ΔW = weight loss (%)

Wo = initial rebar mass (g)

W = rebar mass after rust removal (g)

Ws = amount of uncorroded part dissolved (g)

4. Results and discussion

4.1 Half-cell potential

Fig. 4 shows the half-cell potentials of anodic bars in cracked parts and cathodic bars in sound parts at the end of 105 high temperature/humidity and low temperature/humidity cycles. The bold line in the figure represents a potential of −0.35 V (vs. CSE), at which the probability of corrosion is 90% by the corrosion criter ia of ASTM C 876-80.[14] This figure reveals that the half-cell potentials of both anodic areas of carbonation-induced cracking and cathodic areas in sound parts become less negative as the Cr content of rebars increases. In anodic areas, potentials less negative than −0.35V are measured only on rebars with Cr content of 5% or more, whereas such values are recorded on all rebars in cathodic areas. Note that the potential differences between anodic and cathodic areas is rather large for rebars with a Cr content of 5% or less but the difference is hardly noticeable for rebars with Cr content of 7% or more.

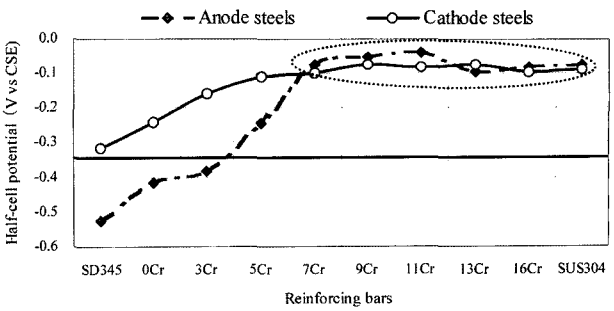

Fig. 4 Half-cell potentials of anodic bars and cathodic bars at the end of 105 high temperature/high humidity and low temperature/low humidity cycles.

4.2 Time-related changes in macrocell corrosion current density

Fig. 5 shows the time-related changes in the carbonation-induced macrocell corrosion current density of each steel type. The macrocell corrosion current density was determined by dividing the measured macrocell corrosion current by the surface area of anodic bars. In this study, a corrosion current density of 0.2 μA/cm^2 was adopted as the criterion for judging the onset of macrocell corrosion. This value corresponds to a minute current level in Cr-bearing corrosion resistant rebars in a passive state (passive state retention current) adopted based on previous papers.[15-18] If the measured macrocell corrosion current density was 0.2 μA/cm^2 or less, then it was determined that no macrocell corrosion was occurring. According to Fig. 5, the macrocell corrosion current density tends to be higher in Cr-bearing rebars with a lower Cr content. Notice that the macrocell corrosion current density tended to decrease over time during accelerated corrosion curing regardless of the steel bar type. This can be attributed to the corrosion products accumulating on anodic bars, which inhibited the diffusion of iron ions and dissolved oxygen while increasing the electric resistance[19-21]. On the other hand, macrocell corrosion current density of SD345 were 0.2 mA/cm^2 or more. Then again, the measured macrocell corrosion current density of rebars with a Cr content of 3% were 0.2 mA/cm^2 or less. The macrocell current densities of Cr-bearing rebars with Cr content of 5% or more were particularly marginal.

4.3 State of rebar corrosion

The state of rebar corrosion on anodic bars in cracked parts is shown in Fig. 6 . This figure reveals that corrosion tends to be

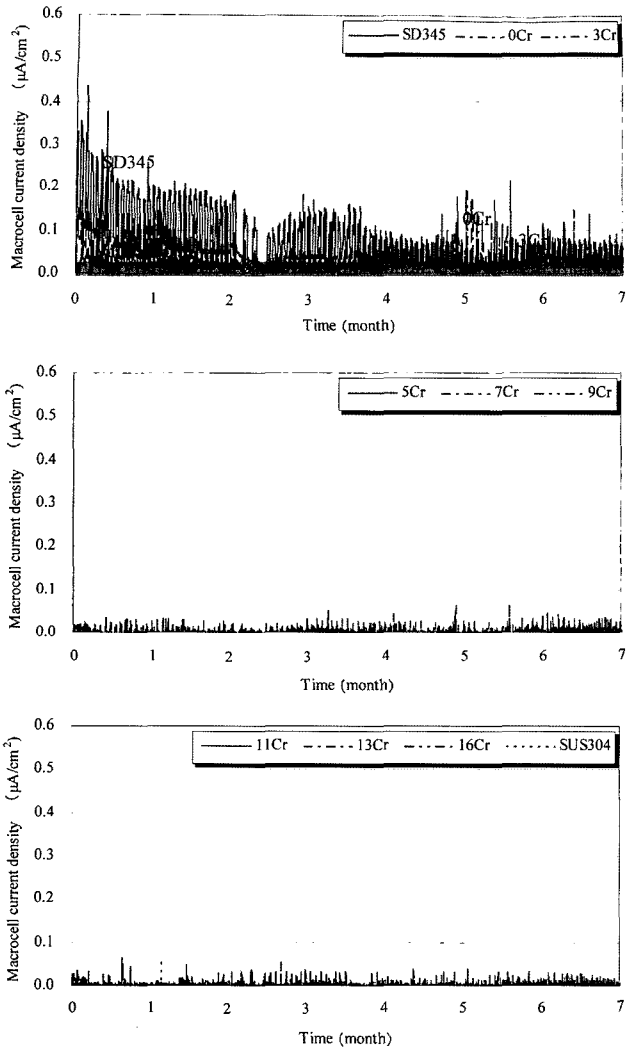

Fig. 5 Time-related changes in the carbonation-induced macrocell corrosion current density of each steel bar type.

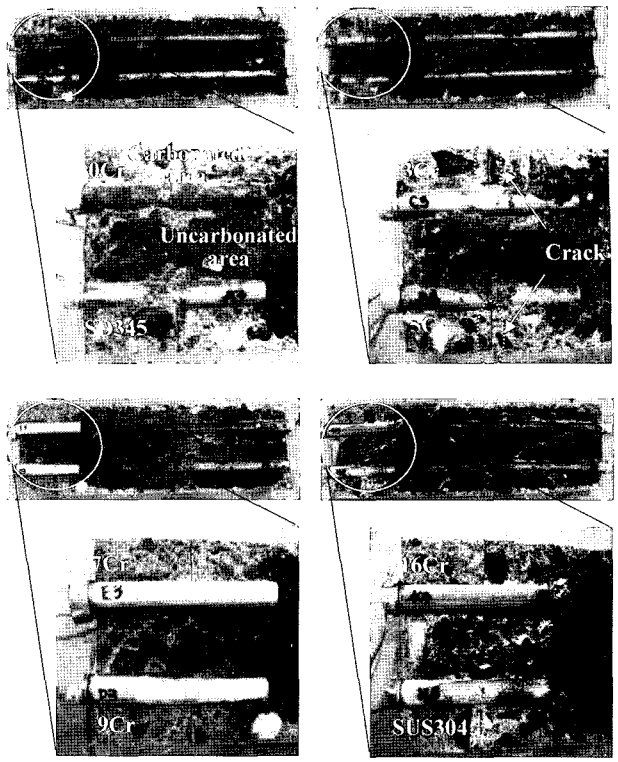

Fig. 6 State of rebar corrosion of cracked parts on anodic bars.

more significant on rebars with lower Cr content. Corrosion was visible on rebars with Cr content of 3% or less and particularly significant on SD345, but it was scarcely observed on rebars with Cr content of 5% or more. On the other hand, carbonation was found to spread not only in the area near the cracking but also over the entire anodic surfaces of rebars presumably because CO_2 seeping through cracking has readily migrated along the rebar-concrete interfaces into sound cover concrete near the anodic rebars. In cathodic areas, however, carbonation was found to remain near the concrete surfaces without reaching the rebar level. Such intensive carbonation near the cracks has caused differences in the pH values of anodic and cathodic bars, forming a macrocell corrosion environment as intended in this study.

4.4 Corrosion area

The corrosion areas of cracked part on anodic bars and of sound (uncracked) parts on cathodic bars at the end of 105 cycles of accelerated corrosion curing consisting of high temperature/high humidity and low temperature/low humidity phases are depicted in Fig. 7. This figure reveals that the corrosion area tends to decrease as the Cr content increases, and this tendency is more noticeable in anodic areas. According to the above Section 4.2 (Time-related changes in macrocell corrosion current density) of this paper, marginal macrocell corrosion current densities below 0.2 mA/cm^2 were recorded on rebars with Cr content of 5% or more. It is therefore inferred that it is necessary for the steel bars to have the Cr content of at least 5% to suppress the corrosion in a macrocell corrosion environment induced by intensive carbonation of cracked parts. Yet, according to Fig. 7, corrosion areas of approximately 5% were observed on 5Cr rebars. This can be attributed to microcell corrosion, which is normally associated with macrocell corrosion of cracked areas. On the other hand, there was no area of corrosion for rebars with Cr content of 7% or more.

4.5 Corrosion loss

Fig. 8 shows the corrosion losses of anodic and cathodic rebars at the end of 105 cycles of accelerated corrosion curing consisting of high temperature/high humidity and low temperature/low humidity phases. Similar to the above-mentioned corrosion area results, the corrosion losses tend to decrease as the Cr content increases, and no corrosion is observed on anodic with Cr contents of 7% or more and on cathodic bars with Cr contents of 5% or more.

These results of half-cell potential, macrocell corrosion current density, corrosion area, and corrosion loss indicate that it takes Cr-bearing steel bars with Cr content of 5% or more to suppress the corrosion in a macrocell corrosion environment induced by the differences in pH values due to the carbonation of cracked parts. However, small rusts presumably due to microcell corrosion were observed on 5Cr steel containing 5% Cr. 5Cr steel is therefore found corrosion-resistant up to the age corresponding to 105 cycles of the present accelerated corrosion testing. However, it is not deemed sufficiently resistant to the level of long-life structures with an expected service life of over 100years. On the other hand,

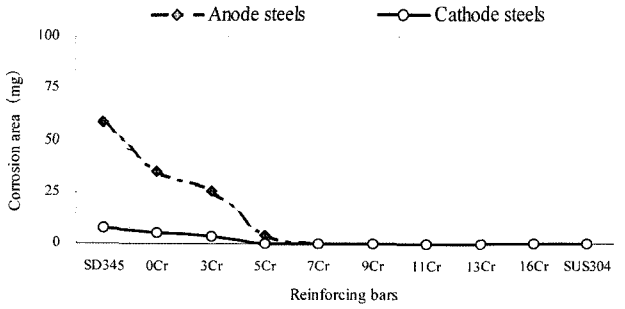

Fig. 7 Corrosion areas on anodic bars and cathodic bars at the end of 105 high temperature/humidity and low temperature/humidity cycles.

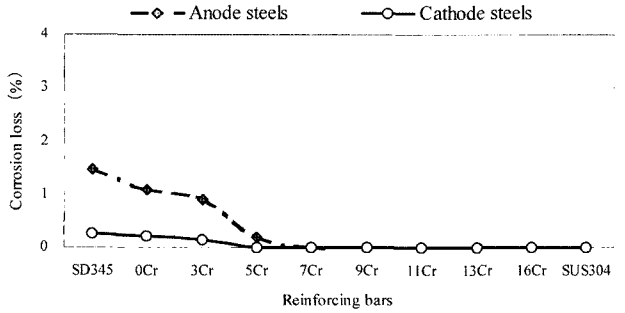

Fig. 8 Corrosion losses of anodic and cathodic rebars at the end of 105 high temperature/humidity and low temperature/humidity cycles.

Cr-bearing steels with a Cr content of 7% or more are proven to possess excellent corrosion resistance, as the potential differences between their anodic and cathodic areas are marginal. Their measured macrocell corrosion current density was far lower than 0.2 mA/cm^2. Moreover, their corrosion areas and corrosion losses were both 0%.

5. Conclusions

In this study, the corrosion-inhibiting properties of Cr-bearing rebars under a macrocell corrosion environment induced by cracking in cover concrete were investigated.

As the result, the following conclusions were drawn:

1) The corrosion resistance of steels in a macrocell corrosion environment induced by the differences in the pH values due to carbonation of cracked parts increased as their Cr content increased.

2) In a macrocell corrosion environment induced by localized carbonation, the minimum Cr content of rebars required for corrosion resistance was 5%. The corrosion-resisting performance of Cr-bearing rebar was particularly noticeable with Cr content of 7% or more.

Acknowledgements

This work is a part of the study supported by JFE Steel Corporation (former Kawasaki Steel Corporation). It is also supported by the SRC/ERC program of MOST (Grant # R11-2005-056-01003-0).

References

1. Gowripalan, N., Sirivivatnanon, V., and Lim, C. C., "Chloride diffusivity of concrete cracked in flexure," *Cement and Concrete Research*, Vol.30, 2000, pp.725~730.

2. Lorentz, T. and French, C., "Corrosion of reinforcing steel in concrete:Effects of materials, mix composition, and cracking," *ACI Materials Journal*, Vol.92, No.2, March-April, 1995, pp.181~190.

3. Otsuki, N., Miyazato, S., Diola, N., and Suzuki, H., "Influence of bending crack and water-cement ratio on chloride-induced corrosion of main reinforcing bars and stirrups," *ACI Materials Journal*, Vol.97, No.4, July-August, 2000, pp.453~462.

4. Raupach, M., "Chloride-induced macrocell corrosion of steel in concrete-theoretical background and practical consequences," *Construction and Building Materials*, Vol.10, No.5, 1996, pp.329~338.

5. Kobayashi, K. and Miyagawa, T., "Numerical analysis of corrosion rate of steel bar suppering from macro-cell corrosion using polarization resistance," *Fourth Int. Conf. of Concrete under Severe Conditions of Environment and Loading (Consec04)*, Vol.1, 2004, pp.249~256.

6. Schie, P. and Raupach, M. l., "Laboratory studies and calculatins of the influence of crack width on chloride-induced corrosion of steel in concrete," *ACI Materials Journal*, Vol.94, No.1, January-February, 1997, pp.56~62.

7. Treece, R. A. and Jirsa, J. O., "Bond Strength of Epoxy-Coated Reinforcing Bars," *ACI Materials. Journal*, Vol.86, No.2, March-April, 1989, pp.167~174.

8. Miura, T. H. and Itabashi, I. I., "Study on Allowable Coating Damage of Epoxy-Coated Reinforcing Bars," *ACI Materials. Journal*, Vol.94, No.4, July-August, 1997, pp.267~272.

9. Smith, F. N. and Tullmin, M., "Using Stainless Steels as Long-Lasting Rebar Material," *Materials Performance*, May, 1999, pp.72~76.

10. Rostam, S., "Reinforced concrete structures-shall concrete remain the dominating means of corrosion prevention?," *Materials and Corrosion*, Vol.54, 2003, pp.369~378.

11. Borges, P. C., Rincon, O. T., Moreno, E. I. and A, A. "Torres-Acosta, M. Martinez-Madrid, A. Knudsen, Performance of a 60-Year-Old Concrete Pier with Stainless Steel Reinforcement," *Materials Performance*, October, 2002, pp.50~55.

12. Tae, S. H., Noguchi, T. and Ujiro, T., "Corrosion Behavior of Cr-bearing Rebar in Concrete with Chloride Ion Content," *Journal of the Architectural Institute of Korea*, Vol.7, June, 2005, pp.49~54.

13. Japan Concrete Institute, *Examination method and criterion about corrosion, corrosion resistance of a concrete construction (plan)*, JCI-SC1, corrosion evaluation method of steel materials in concrete, 1987, pp.1~2.

14. ASTM C 876-80, *Standard test method for half cell potentials of reinforcing steel in concrete*, 1981, pp.554~560.

15. Lopez, W. Gonzalez, J. A., and Andrade, C., "Influence of temperature on the service life of rebars," *Cement and Concrete Research*, Vol.23, 1993, pp.1130~1140.

16. Alonso, C. and Andrade, C., "Effect of nitrite as a corrosion inhibitor in contaminated and chloride-free carbonated mortar," *ACI Materials Journal*, Vol.87, No.2, March-April,

1990, pp.130~137.

17. Yamaji, T., Aoyama, T., Yamagawa, M., and Simizu, T., "Corrosion property of a Stainless steel rebar in the concrete inside," *Proceedings of the Concrete Structure Scenarios JSMS, Kyoto,* Vol.1, 2001, pp.69~74. (Japanese)

18. Erdogdu, S., Bremner, T. W., and Kondratova, I. L., "Accelerated testing of plain and epoxy-coated reinforcement in simulated seawater and chloride solutions," *Cement and Concrete Research,* Vol.31, 2001, pp.861~867.

19. Liu, T. and Weyers, R. W., "Modeling the dynamic corrosion process in chloride contaminated concrete structures," *Cement and Concrete Research,* Vol.28, No.3, 1998, pp.365~379.

20. Yalcyn, H. and Ergun, M.,"The prediction of corrosion rates of reinforcing steels in concrete," *Cement and Concrete Research,* Vol.26, No.10, 1996, pp.1593~1599.

21. Arya, C. and Vassie, P. R. W., "Influence of cathode-to-anode area ratio and separation distance on galvanic corrosion currents of steel in concrete," *Cement and Concrete Research,* Vol.25, No.5, 1995, pp.989~998.